S1 Supplementary Material

S1.1 Temporal stability of opacitiy-induced effects

An additional aspect to be discussed is the response time of the atmospheric system to the imposed cloud modifications. To investigate this we use experiments, in which $f_{op} = 0.1$ is applied as in EXPL for the first 4 days but then switched off for 6 more days of simulation time. Control runs with $f_{op} = 1.0$ for all times were produced for comparison. As in EXPL, simulations were started every 4th day but run out to 10 days and two starting dates in August were added (3rd and 7th of August) to give better statistics for the time evolution. Figure S1 shows box-averaged 10-day time-series of RR, cover of low clouds CLC_{low} and that of high clouds CLC_{high} (below 800 hPa and above 400 hPa, respectively) for the DACCIWA region (Figs. S1a–c). The corresponding differences between the two sets of simulations are provided in the right-hand side panels of Fig. S1.

After the switch-off at 12 UTC on the fifth simulation day (i.e. after 96 hours), the differences in SSI and low-level T are reduced almost immediately (not shown), but for other variables the response is slower. RR shows the enhancement of afternoon and evening precipitation for $f_{op} = 0.1$ as in EXPL (Figs. S1a and f). The enhancement is still fully visible for the first 14 hours after switch-off, indicating that the influence of the forcing during the morning hours is already enough to generate more instability and trigger more convection later in the day. After that, differences between the two runs become negligible. Before the switch in f_{op}, CLC_{low} shows the familiar afternoon decrease and nighttime increase (Figs. S1b and g). On the day of the change, some signal remains until the morning of the following day, similar to RR. The small but on average slightly positive differences after that may be a reflection of increased surface fluxes after the strongly enhanced rainfall of the first five days. CLC_{high} (Figs. S1c and h) shows a considerably slower response. Differences between the two runs need one full diurnal cycle to establish and are then positive for the next three days. After the switch, there is a marked decrease in differences but then an overall tendency for relatively large values for two more days. This is consistent with Raymond et al. (2011), who show a considerably longer response time in the tropical upper troposphere than at low levels for a given perturbation.

Another interesting question is the impact on regions to the north, i.e. downstream of the DACCIWA box with respect to the monsoon flow. Figures S1d, e, i and j show corresponding plots for RR over the Sahelian regions 10–15°N and 15–20°N, both averaged over 8°W–8°E. For the former, again an initial response time of about one day is observed followed by a period of small positive differences. During the last five days of the simulation there is then no clear net difference between the two sets of experiments but much larger fluctuations. As these do not follow a strict diurnal cycle, we speculate that this is mostly a reflection of the overall chaotic nature of the atmosphere growing with leadtime. This conclusion is consistent with the similar behavior found for the 15–20°N band.

So in summary, this experiment shows that low-level variables such as SSI and T react almost immediately to changes in low cloud during the day. Low-level cloud cover and rainfall respond after one full diurnal cycle, while upper-level variables and neighboring regions show even longer responses but also increasingly chaotic behavior.

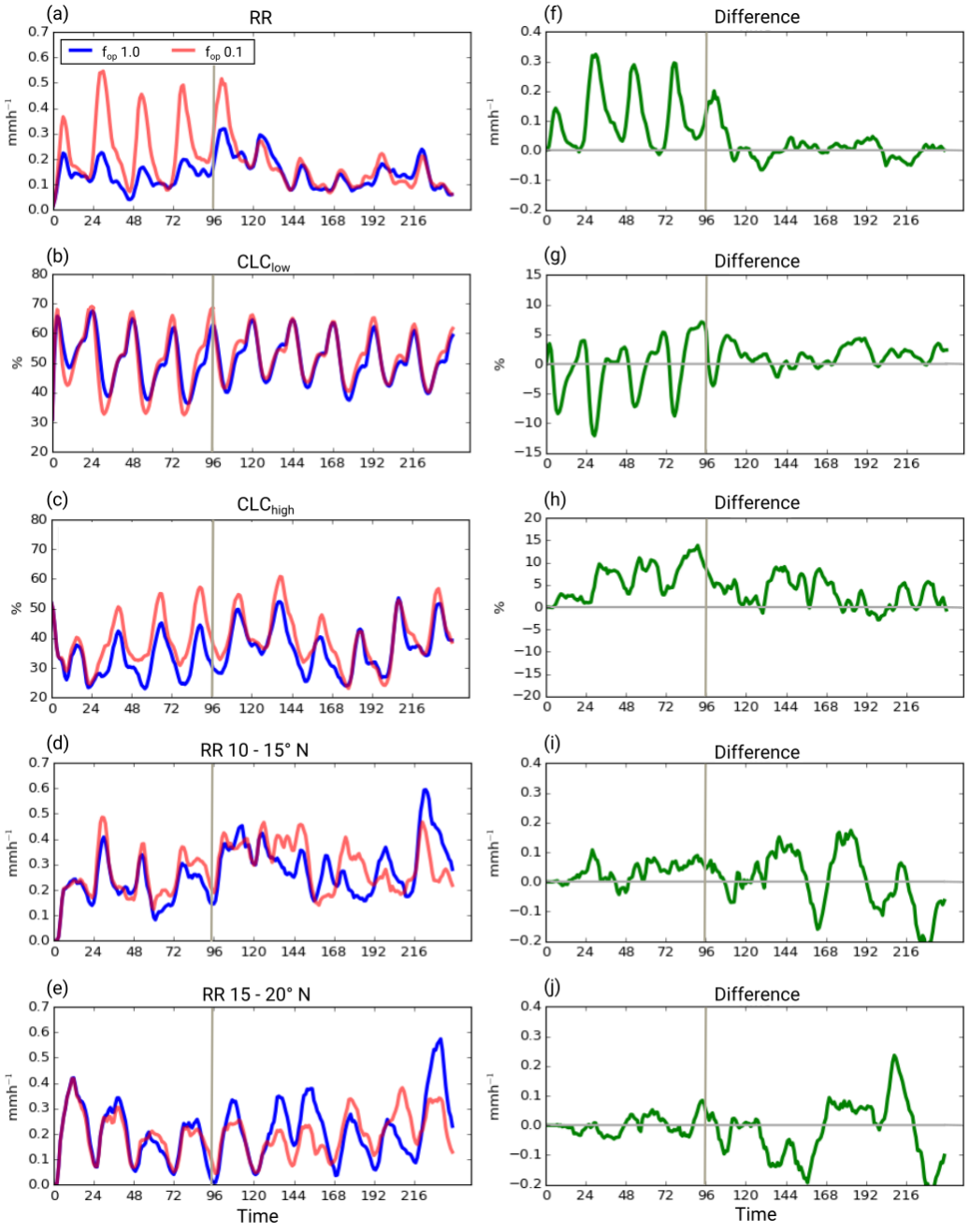

Figure S1. Time-series of RR (a), CLC_{low} (b) and CLC_{high} (c) of the experiments with $f_{op} = 1.0$ all the time (blue line) and f_{op} switched from 0.1 to 1.0 after 96 hours (orange line). Results are averaged over the DACCIWA box, for all 10 runs in July-August 2006. (d) and (e) depict similar averages of RR but for the northern boxes 15–20°N, 8°W–8°E and 15–20°N, 8°W–8°E, respectively. The corresponding differences are shown as green lines in (f)–(j). Switch-off time is indicated by a grey line in all panels.

S1.2 Table of acronyms

Table S1. Table of acronyms and abbreviations used in the main article.

Acronym	denotation
θ_e	equivalent potential temperature
CALIPSO	Cloud-Aerosol Lidar and Infrared Pathfinder Satellite Observation
CERES	Clouds and the Earth's Radiant Energy System
CM SAF	Satellite Application Facility on Climate Monitoring
CLC	cloud cover
CLC_{low}	low-cloud cover
CLC_{high}	high-cloud cover
CloudSat	satellite in A-train with cloud profiling radar
COSMO model	Consortium for Small-scale Modeling model
COSMO-EU	regional COSMO model for Europe
DACCIWA	Dynamics-Aerosol-Chemistry-Cloud Interactions in West Africa project
DWD	German weather service
EBAF-Surface	Energy Balanced And Filled surface irradiance
EBAF-TOA	Energy Balanced And Filled top of atmosphere irradiance
ECMWF	European Centre for Medium-Range Weather Forecasts
ERA-I	ERA Interim
EXPL	experiment with explicit convection
f_{op}	opacity factor
GERB	Geostationary Earth Radiation Budget
GPCP	Global Precipitation Climatology Project
GPCC	Global Precipitation Climatology Centre
ICON	Icosahedral Non-hydrostatic (numerical weather prediction model of DWD)
IFS	Integrated Forecasting System
ITD	Intertropical Discontinuity
MODIS	Moderate Resolution Imaging Spectroradiometer
MPI-M	Max Planck Institute for Meteorology
MVIRI	Meteosat Visible and Infrared Imager
NLLJ	nocturnal low-level jet
NPP	Suomi National Polar-orbiting Partnership
NWP	numerical weather prediction
OLR	outgoing longwave radiation

Acronym	denotation
OSR	outgoing shortwave radiation
p_{sfc}	surface pressure
PARAM	experiment with parameterised convection
PBL	planetary boundary layer
q_c	cloud liquid water content
q_i	cloud ice content
q_v	specific humidity
RH	relative humidity
RR	precipitation rate
RRTM	Rapid Radiation Transfer Model
SARAH	Surface Solar Radiation Data Set Heliosat
SEVIRI	Spinning Enhanced Visible and InfraRed Imager
SLEVE	smooth level vertical (coordinate)
SLI	surface longwave irradiance
SOCRATES	Suite Of Community RAdiative Transfer codes based on Edwards and Slingo
SSI	solar surface irradiance
SST	sea surface temperature
SWA	southern West Africa
SWITCH	experiment where opacity factor is switched to 1 after some time
T	temperature
TERRA	soil and vegetation model
TKE	turbulent kinetic energy
TMPA	TRMM Multisatellite Precipitation Analysis
TOA	top of atmosphere
TRMM	Tropical Rainfall Measuring Mission
v_{horiz}	horizontal wind speed
WAM	West African monsoon